




Article

The Impact of Frequency Support by Wind Turbines on the Small-Signal Stability of Power Systems

Antonio Pepiciello ^{1,*} , José Luis Domínguez-García ¹  and Alfredo Vaccaro ² 

¹ Catalonia Institute for Energy Research (IREC), Jardins de les Dones de Negre 1, Sant Adria de Besos, 08930 Barcelona, Spain

² Department of Engineering, University of Sannio, Piazza Roma 21, 82100 Benevento, Italy

* Correspondence: apeciciello@irec.cat

Abstract: Rising wind energy integration, accompanied by a decreasing level of system inertia, requires additional sources of ancillary services. Wind turbines based on doubly fed induction generators (DFIGs) can provide inertial and primary frequency support when equipped with specific controls. This paper investigates the effect of frequency support provision by DFIGs on the small-signal stability of power systems. To this end, a modified version of the Kundur two-area test system is employed to analyze different scenarios. Wind energy generation is either added to the existing system or displaces part of the synchronous generation. Simulations show that primary frequency support tends to improve the damping of electromechanical oscillations and deteriorate it for converter control-based ones. On the other hand, the inertial response depends on the control parameters.

Keywords: small-signal stability; wind power generation; doubly fed induction generator (DFIG); inertia; transient stability; oscillation damping



Citation: Pepiciello, A.;

Domínguez-García, J.L.; Vaccaro, A.

The Impact of Frequency Support by Wind Turbines on the Small-Signal Stability of Power Systems. *Energies* **2022**, *15*, 8470. <https://doi.org/10.3390/en15228470>

Academic Editor: Surender Reddy Salkuti

Received: 7 October 2022

Accepted: 8 November 2022

Published: 13 November 2022

Publisher's Note: MDPI stays neutral with regard to jurisdictional claims in published maps and institutional affiliations.



Copyright: © 2022 by the authors. Licensee MDPI, Basel, Switzerland. This article is an open access article distributed under the terms and conditions of the Creative Commons Attribution (CC BY) license (<https://creativecommons.org/licenses/by/4.0/>).

1. Introduction

Wind energy capacity has been growing exponentially over the last decade, as carbon neutrality became a crucial goal for policymakers worldwide. This radical transition from centralized and dispatchable power plants to decentralized and stochastic renewable energy sources poses unprecedented challenges to power systems [1].

Doubly fed induction generators (DFIGs) are expected to play a key role in many countries' grid integration targets. However, due to their operating differences with synchronous generators, they raise concerns about power system operation.

The first impact is associated with the location of the DFIGs, strictly related to the presence of wind, their primary energy source. Such locations are different from current power plants, resulting in the modification of power flow paths and their resulting synchronizing and damping forces. More importantly, the reduction in synchronous generation as wind integration displaces less efficient power plants involves operating power systems with lower levels of inertia. Indeed, DFIGs cannot provide a natural inertial response since they are decoupled from the grid by power electronic converters.

Other consequences of large wind integration are the reduced number of power system stabilizers (PSSs) on the network and fewer resources providing ancillary services, such as frequency and voltage regulation. Furthermore, DFIGs do not sense the fluctuations in frequency caused by a contingency on the network, and they do not currently provide the same ancillary services as thermal and hydroelectric power plants [2].

A possible solution is equipping DFIGs with appropriate controls for the provision of an emulated inertial response and primary frequency support [3], as expected from the evolving grid codes worldwide [4].

The concept of wind turbines providing frequency support was introduced by the authors of [5], which showed how controls based on frequency deviation and the rate

of change of frequency (ROCOF) can improve the frequency stability of a system. The authors of [6] described how active power from wind turbines can be controlled similarly to synchronous generators. Further works focused either on emulated inertia or primary frequency response, such as [7,8], providing different control alternatives. Finally, the effect of frequency support provision by wind farms on the ROCOF and frequency nadir was assessed in [9,10].

Although it is well known that the lack of synchronous inertia from wind farms negatively affects the frequency response of the system after a contingency [11], the results for small-signal stability analysis and low-frequency oscillation damping are still ambiguous.

The effect of the dynamic interaction between DFIGs and power systems on small-signal stability is demonstrated by [12], which explored the modal coupling of control loop models. According to the same author, the impact of DFIGs on low-frequency oscillation damping depends on the test systems and their operating conditions [13]. For example, the authors of [14] stated that the introduction of DFIGs can have either positive or negative effects on damping, depending on the sensitivity to system parameters such as the power flows, location of the wind farms and load conditions. A discussion on how reactive power control strategies affect oscillation damping is reported in [15], where the authors concluded that controlling the terminal voltage instead of providing a fixed amount of reactive power can be more beneficial in terms of damping. In [16], the effect of a wind farm's location on inter-area oscillations was explored, and it was shown that the changes in damping appear to be negligible, although damping is slightly worsened when the wind farm is in the importing area. In order to distinguish the impact of load flow changes and dynamic interactions introduced by DFIGs, in [17], a method based on damping torque analysis for the separate examination of these two affecting factors is proposed. Finally, the analysis carried out in [18] showed that the effects of DFIGs on small-signal stability can also be assessed by data-driven methods, such as power spectral density analysis.

Equipping DFIGs with PSSs, similar to synchronous generators, might be a successful strategy to improve oscillation damping [19]. Different approaches have been proposed. One possibility is taking local signals from the point of common coupling as an input to the PSS [20]. Another interesting challenge is the optimal selection of the input signal to the PSSs, based on the controllability and observability aspects of the signals [21].

As is clear from this literature review, there is an increasing trend of equipping DFIGs with controls for inertial and primary frequency support provision. Furthermore, additional controls for low-frequency oscillation damping from DFIGs are being proposed. However, little research effort has been devoted to the analysis of the interactions between frequency stability and low-frequency oscillations, which are strictly intertwined. The first results on the optimization of a DFIG's fast frequency response, accounting for small-signal stability constraints, are presented in [22]. Furthermore, the authors of [23] analyzed the impact of frequency support provision by direct drive, full-converter-based wind farms on small-signal stability and concluded that ancillary frequency control has a beneficial effect on low-frequency oscillation damping.

The effect of inertial response provision from DFIGs on small-signal stability was investigated by [24], and the authors concluded that the effect can be either positive or negative, depending on the control parameters. However, the intertwining effects between inertial and frequency support and the impact on converter-control based oscillations were neglected.

This paper further investigates the effect of primary and inertial frequency provision from DFIGs on small-signal stability by providing new insights into additional aspects of power system stability, particularly electromechanical and converter control based low-frequency oscillations. It is shown that, depending on if the wind farm is added to the system or displaces synchronous generators, the type of DFIG control and the nature of low-frequency oscillations, the inertial and primary frequency support by DFIGs has different impacts. First, this impact is demonstrated through the mathematical analysis of the single machine infinite bus (SMIB). Additional simulations with the Kundur two-area

system are performed to determine the effect of primary frequency support by DFIGs for different scenarios of wind integration. Furthermore, sensitivity analysis on the droop control parameters characterizing the inertial and primary frequency support is carried out to show the impact of parameter selection on low-frequency oscillations.

2. Power System Stability

Power system stability can be defined as the ability of a system to return to an equilibrium point after a disturbance. It can be classified according to the observed variables and the magnitude of disturbance in the rotor angle, voltage and frequency stability. The classification was recently revised to take into account the contribution of converter-interfaced generation, introducing the new concepts of converter-driven and resonance stability [25]. This paper addresses the frequency, small-signal rotor angle stability and their mutual interactions when DFIGs provide inertial and primary frequency support to the grid.

2.1. Frequency Stability

Frequency stability refers to the ability of a power system to maintain a steady value for the frequency following a severe system perturbation. It depends on the ability to sustain or restore equilibrium between the system generation and load.

The aggregated second-order dynamic model of a power system (Equation (1)) provides useful insights into frequency stability and the need for frequency support provision [11]:

$$2H_{sys}\ddot{\delta} = P_g + P_{reg}(\delta) - P_l \quad (1)$$

where δ is the rotor angle, H_{sys} represents the total inertia of the system, $f_c = \dot{\delta}$ is the frequency of the center of inertia, P_g is the total generation and P_l is the load. The term P_{reg} is the regulating power, which is a function of the frequency.

In a steady state, the total generation is equal to the total load. However, when the equilibrium is perturbed, the frequency deviates from the nominal value. This causes the inertial response of synchronous generators, which has a stabilizing effect on the grid. The inertial response is followed by the primary control, whose aim is to bring the system back to an equilibrium point through $P_{reg}(f_c)$. DFIGs do not provide a natural inertial response, but appropriate control loops can be implemented in the power converters to provide both inertial and primary frequency support, contributing to the regulating power $P_{reg}(f_c)$.

2.2. Small-Signal Stability

Small-signal stability refers to the transient behavior of power systems, induced by small perturbations around an equilibrium point.

An operating point is considered stable if and only if all eigenvalues of the linearized model of the power system have a negative real part. A damping ratio ζ_i , calculated through Equation (2), can be associated with each complex eigenvalue $\lambda_i = \alpha_i + j\beta_i$, which represents an oscillating mode:

$$\zeta_i = \frac{-\alpha_i}{\sqrt{\alpha_i^2 + \beta_i^2}} \quad (2)$$

The damping ratio is a useful index to assess how close to instability each oscillating mode is. A mode can be defined as critical if $\zeta_i \leq 5\%$ [26].

Depending on their frequency, electromechanical oscillating modes in power systems can be distinguished into local, if their frequency is around 2 Hz and inter-area, characterized by a lower frequency from 0.1 to 1 Hz.

As observed in [27], the integration of converter-interfaced generation introduces oscillating modes whose frequencies are similar to both inter-area and local modes, although they depend on control systems, and their physical nature is not electromechanical.

Participation factors are used to distinguish electromechanical modes from converter control-based ones. The participation factor p_{ik} , which accounts for the participation of the k th state to the i th mode, can be calculated as in Equation (3):

$$p_{ik} = u_{ki}v_{ki} \quad (3)$$

where u_{ki} and v_{ki} are the elements of the modal matrices of the left and right eigenvectors \mathbf{u} and \mathbf{v} , respectively.

Participation factors can be employed to calculate the converter control-based generation participation index (CCBG-PI) introduced in [27].

The CCBG-PI of a mode i can be computed from Equation (4):

$$\text{CCBG-PI}_i = \frac{\sum_k^{\mathcal{N}_{\text{CCBG}}} p_{ki}}{\sum_k^{\mathcal{N}} p_{ki}} \quad \text{for mode } i \quad (4)$$

where $\mathcal{N}_{\text{CCBG}}$ is the set of state variables associated with converter-control based generation only, while \mathcal{N} is the set of all state variables. This index is employed to identify to what extent the dynamics of a converter-interfaced generator impacts the existing modes and to distinguish converter control-based oscillating modes from inter-area and local ones.

3. Frequency Support Provision by DFIGs

During normal operation, DFIG controllers aim at maintaining the turbine at its optimal speed, which is associated with the maximum power extraction from wind [28].

The maximum power is achieved by controlling the rotor speed ω_r and the pitching angle β to maintain the aerodynamic power efficiency C_p at its optimal value. This control scheme is called maximum power point tracking (MPPT) and is represented by the first block of Figure 1: the PI control.

The reference rotor speed $\omega_{m,ref}$ is estimated using the characteristic curve of the wind turbine, and it is used to set the optimal value of the electrical torque reference $T_{\omega,ref}$.

This control system can be enhanced for the emulated inertia and primary frequency control, which are represented by the droop controls in the second and third blocks of Figure 1, respectively. The inertial and primary frequency droop controls, based on the ROCOF $\frac{df}{dt}$ and frequency deviation Δf , add two set points to the optimal point P_{opt} , resulting from the MPPT. The inertial control is proportional to the controller constant K_{in} , the primary frequency control is proportional to K_p , and according to [29], they can be optimally tuned. The complete control scheme, shown in Figure 1, is illustrated numerically by Equation (5). Additional details on the $P - \omega$ curve can be found, for example, in [6]:

$$P_{ref} = P_{opt} - K_p \Delta f - K_{in} \frac{df}{dt} \quad (5)$$

The sum of the MPPT, primary and inertial droop control sets the reference power P_{ref} required by the converter controls.

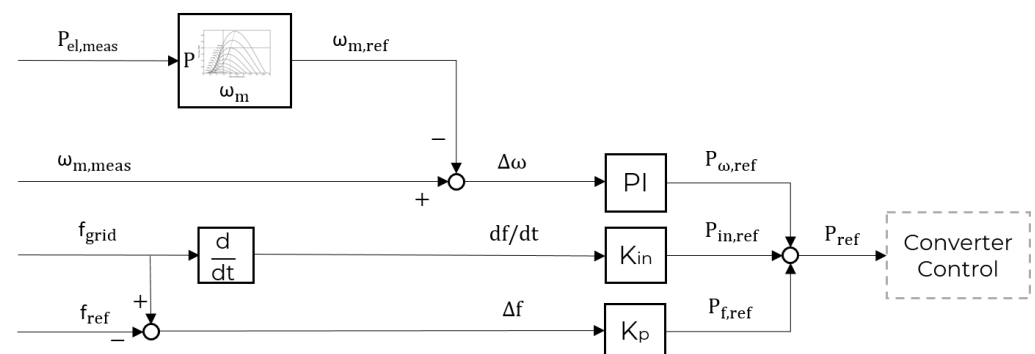


Figure 1. Inertial and primary frequency support control scheme [5].

In order to work properly, the system requires extra energy for regulation. For inertial response, since the control has to be fast, a possible option is extracting the kinetic energy from the rotor [30].

Since wind turbines rotate to convert wind energy, they store a certain amount of it as kinetic energy. Through specific controls, the kinetic energy can be extracted and provided to the system when needed. Available methods to supply inertial and primary frequency support include, among others, kinetic energy extraction, pitch de-loading or accelerative de-loading [31].

Unlike fuel, which is assumed to be always available, wind has an intrinsically stochastic nature, which makes reserve dispatching difficult. This challenge could be managed by associating energy storage systems to the wind farm, providing frequency support so that the service is available even when wind is not [32].

4. Mathematical Insights from SMIB System

The SMIB system is commonly employed in power system stability studies to gain useful mathematical insights about power systems [33]. In this paper, it is used to evaluate mathematically the effect of the inertial and primary frequency control provided by a wind farm on the oscillating modes characterizing the system.

Suppose that we add a wind farm with the droop control described in Figure 1 to the generating bus of the SMIB system. The corresponding linearized equations of the system are shown in Equation (6):

$$\begin{aligned} 2H\dot{\Delta f} &= -K_p\Delta f - K_{in}\dot{\Delta f} - K_S\Delta\delta - K_D\Delta f \\ \dot{\Delta\delta} &= \omega_0\Delta f \end{aligned} \quad (6)$$

where H is the inertia constant of the synchronous generator, K_S the synchronizing coefficient, K_D is the damping coefficient, $\omega_0 = 2\pi f_0$ is the nominal rotor speed and Δf and $\Delta\delta$ are the p.u. frequency and rotor angle deviations, respectively.

Written in matrix form, Equation (6) becomes

$$\begin{bmatrix} \dot{\Delta f} \\ \dot{\Delta\delta} \end{bmatrix} = \begin{bmatrix} \frac{-K_p - K_D}{2H + K_{in}} & \frac{-K_S}{2H + K_{in}} \\ \omega_0 & 0 \end{bmatrix} \begin{bmatrix} \Delta f \\ \Delta\delta \end{bmatrix} \quad (7)$$

The complex conjugate pair of eigenvalues λ_{SMIB} corresponding to this system is equal to

$$\lambda_{SMIB} = -\frac{K_D + K_p}{4H + 2K_{in}} \pm \frac{\sqrt{(K_p + K_D)^2 - 8K_S H \omega_0 - 4K_{in} K_S \omega_0}}{4H + 2K_{in}} \quad (8)$$

The resulting damping ratio from Equation (2) is equal to

$$\zeta = \frac{K_p + K_D}{\sqrt{2(K_p + K_D)^2 - 8K_S H \omega_0 - 4K_{in} K_S \omega_0}} \quad (9)$$

By substituting the values of $K_D = 10$, $K_S = 0.75$, $H = 3.5$ s and $\omega_0 = 2\pi 60$ rad/s from [33], the value of λ_{SMIB} can be plotted for different K_{in} and K_p values to evaluate its sensitivity of the oscillating modes to the inertial and primary responses. Figure 2 shows that the primary response increases the damping of the system, whereas the inertial response may have a negative impact on damping. This result will be confirmed in the case study when assessing the sensitivity of oscillating modes to the inertial and primary droop constant for the Kundur two-area system, a widely employed benchmark system for stability studies.

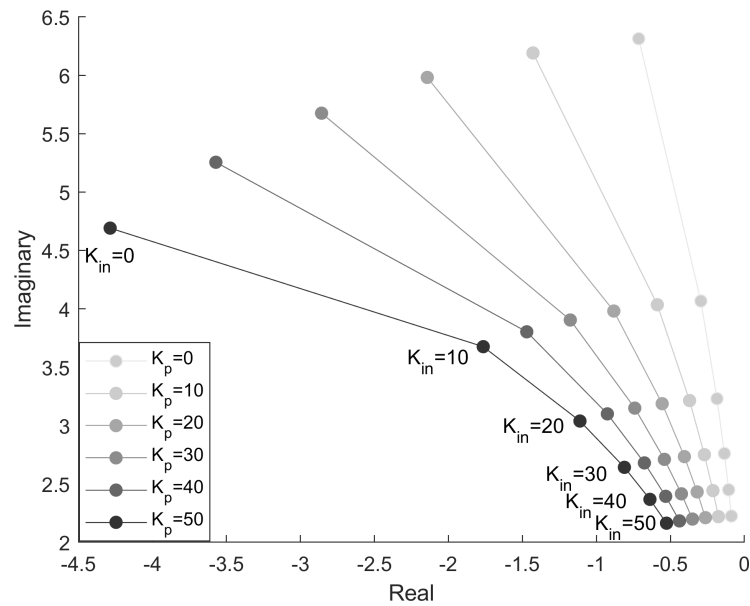


Figure 2. Sensitivity analysis of λ_{SMIB} to K_p and K_{in} .

5. Case Study

In this section, a modified version of the two-area Kundur system [33] including wind generation is analyzed to investigate the effects on small-signal stability of DFIGs providing frequency support to power systems.

The one-line diagram of the system is drawn in Figure 3.

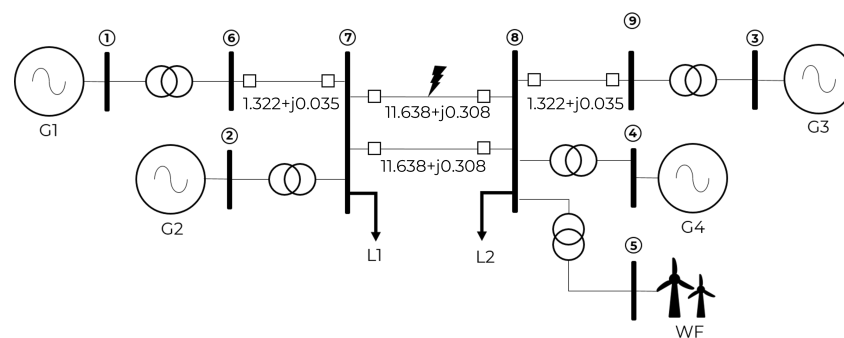


Figure 3. Modified two-area Kundur system.

The original system consists of two areas, each having two synchronous generators. The areas are connected by two parallel HV transmission lines 220 km in length at 230 kV. All synchronous generators were modeled in detail, including prime movers, speed governors, excitation systems and PSSs. Their nominal power was equal to 900 MVA each, and the active power generated in the considered operating condition was around 600 MW. Each area had a single lumped load modeled as constant impedance, and the total load was around 2300 MW. Wind power generation, added at bus 5, is represented by a lumped dynamical model of a wind farm working with DFIG-type turbines.

This model was chosen as it is the most commonly employed one in the literature when evaluating power system small-signal stability. However, more alternative models are available in the literature. For example, coordinated control of both the inertial and primary frequency support is described in [34]. In [35], the model for inertial response includes hybrid energy storage and communication delays. Finally, in [36], the control gains were considered time variant due to the boundary conditions, such as the wind speed.

Its nominal power depends on the scenario considered. The model of a DFIG is represented in Figure 4. It consists of a simplified mechanical model of the turbine, the

asynchronous machine model, rotor- and grid-side voltage source converters (VSCs) and the related controls. The wind speed over the wind farm was assumed to be constant during the observation time interval and spatially uniform [37].

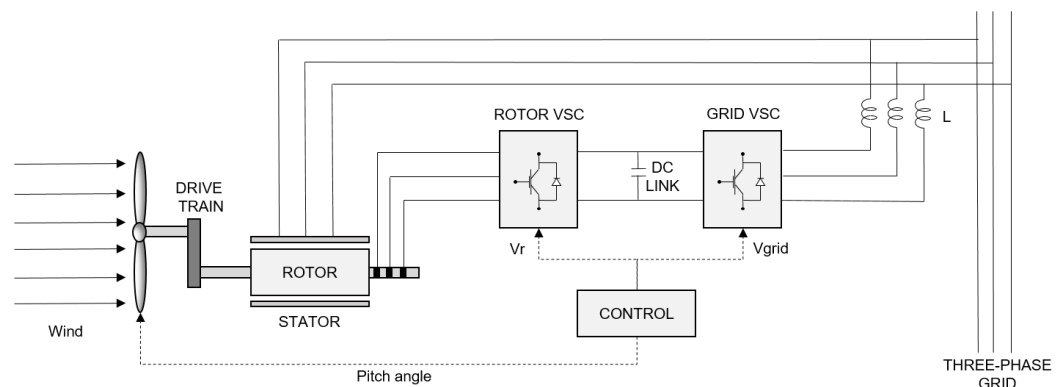


Figure 4. Structure of the DFIG wind turbine model.

For the purpose of this case study, the DFIGs were equipped with the inertial and primary frequency control scheme presented in Figure 1.

The simulation was carried out in MATLAB's Simulink. The starting point was the available classical Kundur two-area system. This system was modified with the addition of a DFIG block together with control blocks to introduce inertial and frequency support capabilities. The small-signal stability analysis was carried out by employing the MATLAB linearization toolbox to calculate the Jacobian matrix and eigenvalues of the dynamical system around the equilibrium point, corresponding to the solution of the power flow. A first case study was carried out considering only primary frequency support provision, followed by a sensitivity analysis on the effects of K_{in} and K_p on low-frequency oscillation damping.

5.1. Impact of Primary Frequency Support Provision by DFIGs

After a critical review of the state of art, the authors of [13] suggested that a complete characterization of the impacts of DFIGs in a power system's small-signal stability analysis should include the following scenarios:

- Scenario A: the initial scenario without the wind farm, corresponding to the classical Kundur two-area system.
- Scenario B: a DFIG-based wind farm is added to the system at bus 5, along with a synchronous generator G_4 . In this case, the nominal power is chosen to be 300 MVA.
- Scenario C: the wind farm displaces the synchronous generator G_4 , and its nominal power is chosen to be around 600 MVA in order to supply the power lacking from G_4 .

In this paper, for each scenario involving the presence of a wind farm, the following sub-scenarios are explored:

- Voltage or reactive power control mode;
- With or without primary frequency support provision.

All the combinations were examined for a total of nine cases, including scenario A.

5.1.1. Scenario A (No Wind)

The analysis of the original two-area Kundur system, without the inclusion of the wind farm, provided an initial understanding of the transient behavior of the system and a foundation to assess the impact of wind farms providing frequency support on low-frequency oscillations. The system parameters were tuned to obtain a loosely damped starting system, which resulted in a more easily observable damping effect of the wind farm. This was achieved by setting the proportional gain of the PSSs to $K_{pss} = 10$.

We started by investigating the small-signal stability of this system. Tables 1 and 2 present four local $\lambda_{l,i}$ and inter-area $\lambda_{ia,i}$ modes, which are the most critical oscillation modes (i.e., the ones closer to the imaginary axis and with the lowest damping ratio).

Table 1. Local modes (scenario A). Bold values highlight critical damping.

	Eigenvalue	Damping	Frequency (Hz)
$\lambda_{l,1}$	$-20.597 \pm 18.900i$	0.736	3.008
$\lambda_{l,2}$	$-18.232 \pm 14.251i$	0.787	2.268
$\lambda_{l,3}$	$-1.026 \pm 8.566i$	0.119	1.363
$\lambda_{l,4}$	$-2.048 \pm 6.578i$	0.297	1.047

Table 2. Inter-area modes (scenario A). Bold values highlight critical damping.

	Eigenvalue	Damping	Frequency (Hz)
$\lambda_{ia,1}$	$-38.981 \pm 1.220i$	0.999	0.194
$\lambda_{ia,2}$	$-25.819 \pm 0.915i$	0.999	0.145
$\lambda_{ia,3}$	$-24.498 \pm 0.801i$	0.999	0.127
$\lambda_{ia,4}$	$-0.046 \pm 2.877i$	0.016	0.458

The inter-area modes appeared to be well damped, excluding $\lambda_{ia,4}$, a critical mode with a very low damping ratio ($\zeta_{ia,4} = 1.6\%$). The local modes were well damped too, with $\lambda_{l,3}$ showing the lowest damping ratio ($\zeta_{l,3} = 11.9\%$). These two modes were the dominant ones, and hence, the following scenarios including wind integration will be focused upon.

The results of the small-signal stability analysis were complemented by a time domain simulation considering a 3-phase fault lasting 10 cycles on the tie line connecting Area 1 and Area 2. The results, in terms of the rotor speeds of the synchronous generators, are shown in Figure 5. The figure shows the generators of Area 1 oscillating against the ones in Area 2, with a frequency around 0.5 Hz, as predicted by the small-signal stability analysis.

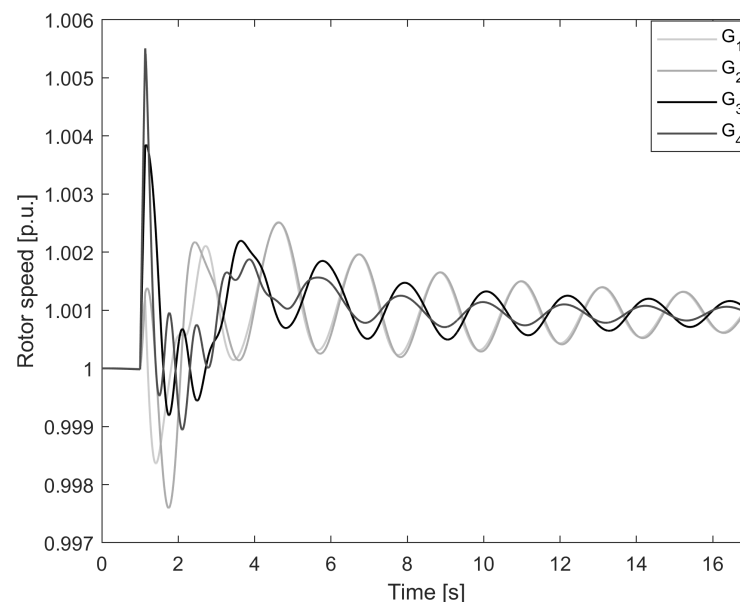


Figure 5. Time domain simulation considering a three-phase fault on the tie line.

5.1.2. Scenario B (Addition of the Wind Farm)

The addition of the wind farm leads to a change in the power flows and to dynamic interactions introduced by the controls of the DFIGs. These joint effects lead to the movement of both local and inter-area modes. Figure 6 illustrates how the oscillating modes changed as the wind farm was added to the system.

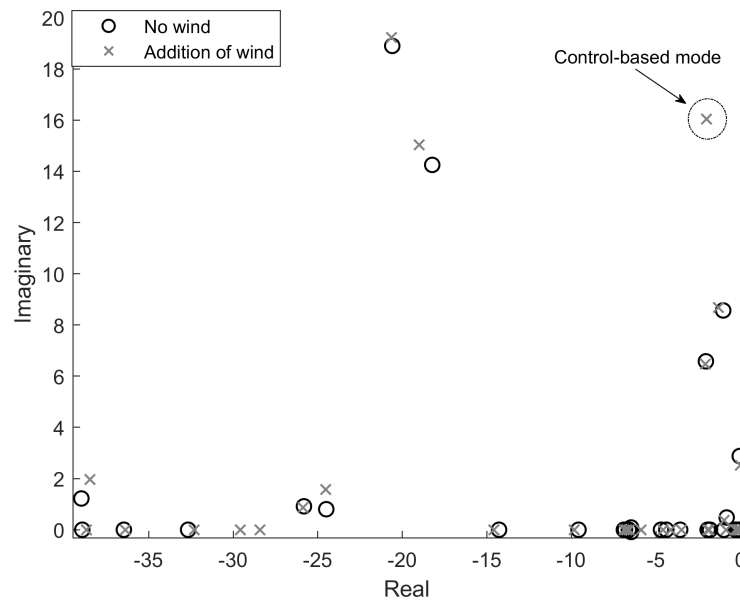


Figure 6. Comparison of eigenvalues between scenarios A and B.

The dynamic interaction of the wind farm was observable through the analysis of the participation factors. Figure 7 shows the participation factors of the inter-area mode $\lambda_{ia,3}$.

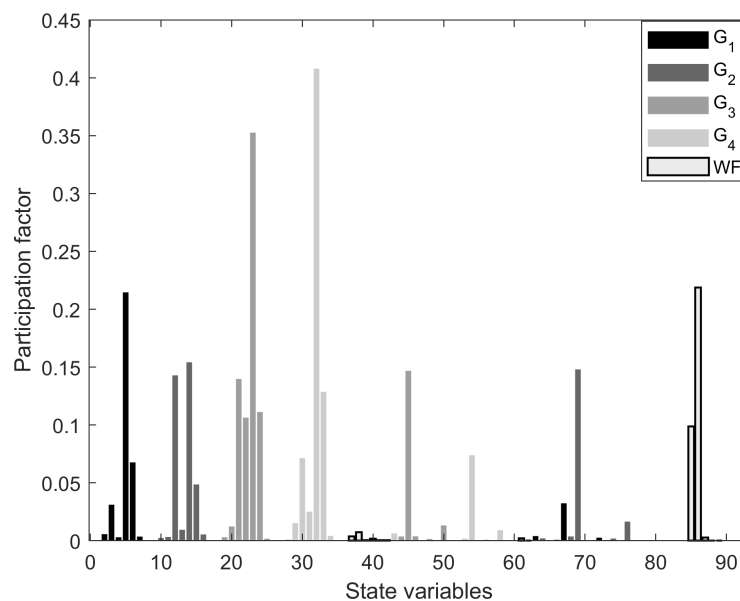


Figure 7. Participation factors associated with the inter-area mode $\lambda_{ia,3}$.

In addition to the participation of all synchronous generators, given its inter-area nature, non-negligible participation of the wind farm was observed, represented by the non-zero values of the participation factors associated with the wind farm state variables. This led to a non-zero (although small) CCBG-PI for $\lambda_{ia,3}$.

An important impact was the emergence of a new oscillating mode in the range of the local modes, which is a converter control-based mode, defined as λ_{cc} . This mode is circled in Figure 6. Its nature can be distinguished from electromechanical modes by the analysis of participation factors and the calculation of the CCBG-PI with (4). The CCBG-PI of λ_{cc} was equal to 98.6%, denoting negligible participation of synchronous generators in this mode. Hence, λ_{cc} was a converter-control based mode.

Table 3 illustrates the numerical values of the dominant inter-area, local and converter control-based modes for the nine cases of interest.

Table 3. Result summary for all scenarios considering dominant inter-area, local and converter control-based modes. The bold and dark gray values highlight the unstable and the most stable case, respectively.

Scenario	Freq. Supp.	Control	Inter-Area Mode		Local Mode		Converter Control-Based Mode		
			Eigenvalue	Damping	Eigenvalue	Damping	Eigenvalue	Damping	CCBG-PI
(A) No wind	-	-	$-0.096 \pm 2.942i$	0.033	$-1.131 \pm 8.757i$	0.128	-	-	-
(B) Add. wind	No f. supp.	V	$-0.008 \pm 2.512i$	0.003	$-1.289 \pm 8.652i$	0.147	$-2.036 \pm 16.093i$	0.125	0.985
		Q	$0.026 \pm 2.342i$	-0.011	$-1.345 \pm 8.601i$	0.154	$-2.013 \pm 15.942i$	0.125	0.985
	F. supp.	V	$-0.069 \pm 2.521i$	0.027	$-1.709 \pm 8.233i$	0.203	$-0.343 \pm 17.204i$	0.019	0.726
		Q	$-0.069 \pm 2.500i$	0.028	$-1.724 \pm 8.199i$	0.206	$-0.328 \pm 17.108i$	0.019	0.723
(C) Displ. G ₄	No f. supp.	V	$-0.459 \pm 3.756i$	0.121	$-1.671 \pm 7.585i$	0.215	$-2.066 \pm 16.009i$	0.128	0.966
		Q	$-0.484 \pm 3.731i$	0.129	$-1.616 \pm 7.589i$	0.208	$-2.218 \pm 16.896i$	0.130	0.963
	F. supp.	V	$-0.694 \pm 2.837i$	0.238	$-1.658 \pm 7.577i$	0.214	$-0.649 \pm 17.696i$	0.037	0.708
		Q	$-0.740 \pm 2.744i$	0.260	$-1.611 \pm 7.579i$	0.208	$-0.529 \pm 18.245i$	0.029	0.722

The addition of the wind farm affected the dominant inter-area mode, whose damping ratio decreased from $\zeta_{ia} = 3.30\%$, corresponding to the case without wind, to $\zeta_{ia} = 0.34\%$ when the wind farm was added and voltage control was employed. The mode crossed the imaginary axis when reactive power control was employed, resulting in the positive real component of the dominant inter-area mode, highlighted in bold in Table 3.

The dominant local mode, on the other hand, improved slightly from $\zeta_l = 12.8\%$ for the scenario without wind to around $\zeta_l = 15\%$ when the wind farm was added.

The converter control-based mode seemed to be well damped with $\zeta_{cc} = 12.5\%$ and did not seem to be affected by the control mode of the DFIGs.

At this point, the primary frequency support provision was added to the wind farm, and its effect on the dominant modes was investigated.

For this scenario, adding the primary frequency support capability increased the small-signal stability of the system. The damping ratio of the inter-area mode increased from $\zeta_{ia} = 0.34\%$ without frequency support to $\zeta_{ia} = 2.80\%$. This value was still lower than the one in the scenario without the wind. However, the frequency support capabilities showed a beneficial effect on the dominant inter-area mode.

Regarding the dominant local mode, the provision of frequency support by the wind farm additionally increased its damping ratio from $\zeta_l = 12.8\%$ in the case without wind to around $\zeta_l = 20.3\%$ when the wind farm providing primary frequency support was added.

An interesting result is associated with the dominant converter control-based mode. Indeed, frequency support appeared to negatively affect its damping ratio, which decreased from $\zeta_{cc} = 12.5\%$ without frequency support to $\zeta_{cc} = 1.90\%$ with frequency support. Furthermore, a decrease in the CCBG-PI when adding the frequency support was observed. This indicates a larger participation of synchronous generators in the converter control-based mode, which may stem from the DFIGs' active power responding to the system's frequency deviations.

The effect of employing voltage or reactive power control appeared to be negligible, being around $\pm 1\%$ of the damping ratios for all the dominant modes. However, the state space plot resulting from the time domain simulation and representing the rotor speed and angle difference between G₂ and G₄ showed that the voltage and reactive power control may have affected the amplitude of the oscillations, as shown in Figure 8.

The time domain simulation, considering a three-phase fault on the tie line as in the previous scenario, showed the impact of frequency support provision on the oscillations. Figure 9 illustrates the rotor speed of a synchronous generator G₃ when wind was added, allowing a comparison of the cases with and without primary frequency support.

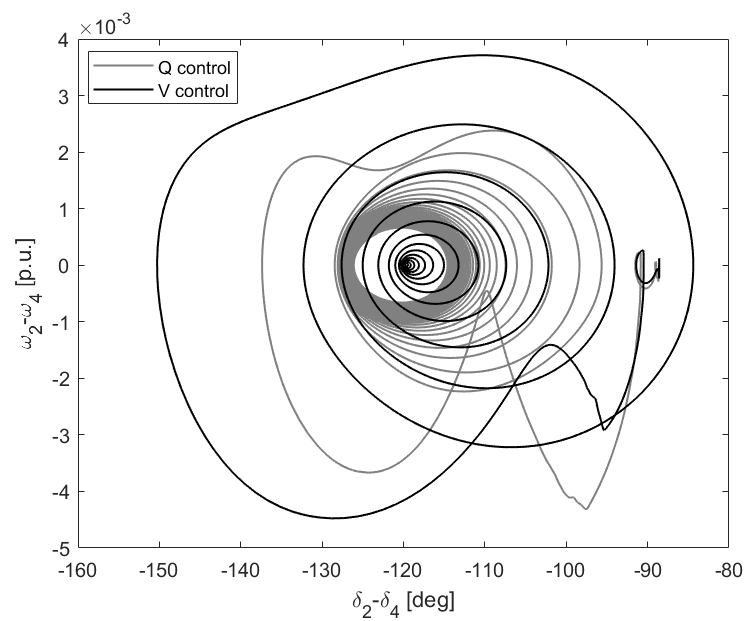


Figure 8. State space from time domain simulation comparing Q and V control.

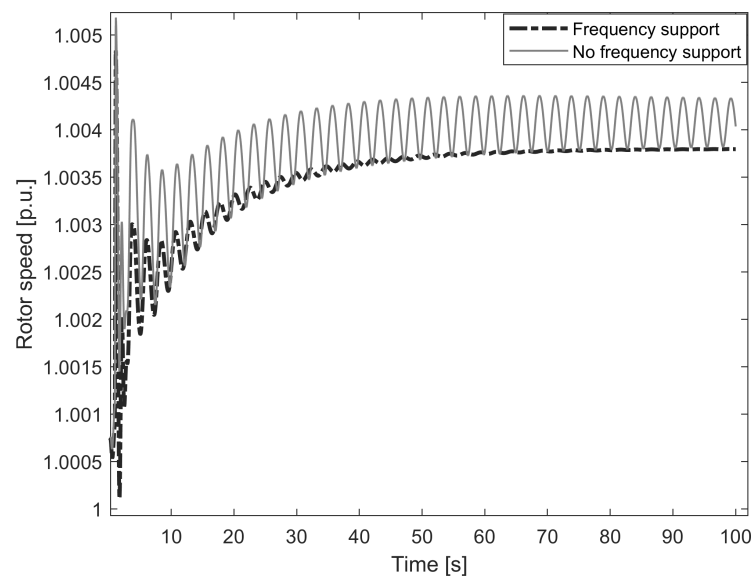


Figure 9. Rotor speed of generator G_3 with and without primary frequency support by a wind farm.

As expected from the eigenvalue analysis, since the dominant inter-area mode was close to a Hopf bifurcation (i.e., it was crossing the imaginary axis), the system suffered sustained oscillations in the scenario with the wind farm without frequency support capabilities. On the other hand, when the wind farm provided primary frequency support, the amplitude of the oscillations was reduced, and they were damped out after a brief time interval. The other synchronous generators, which are not illustrated, showed similar behavior.

Furthermore, different time domain plots for Q and V control of the DFIGs when providing frequency support are shown in Figure 10. As previously seen in the state space representation, the V control led to faster damping of the oscillations. This effect may be due to the fact that with the V control, the DFIGs could provide reactive power to the system, as shown in Figure 11, since it was not constrained to a certain set point.

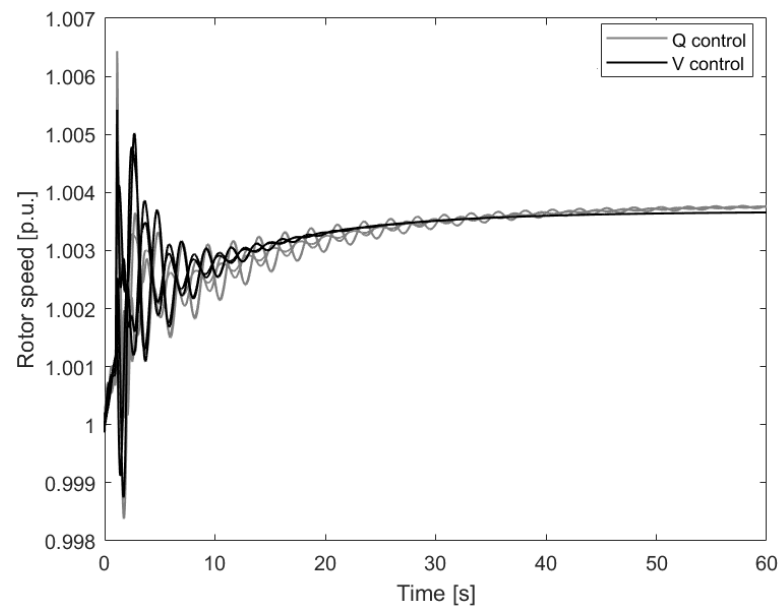


Figure 10. Time domain simulation comparing Q and V control.

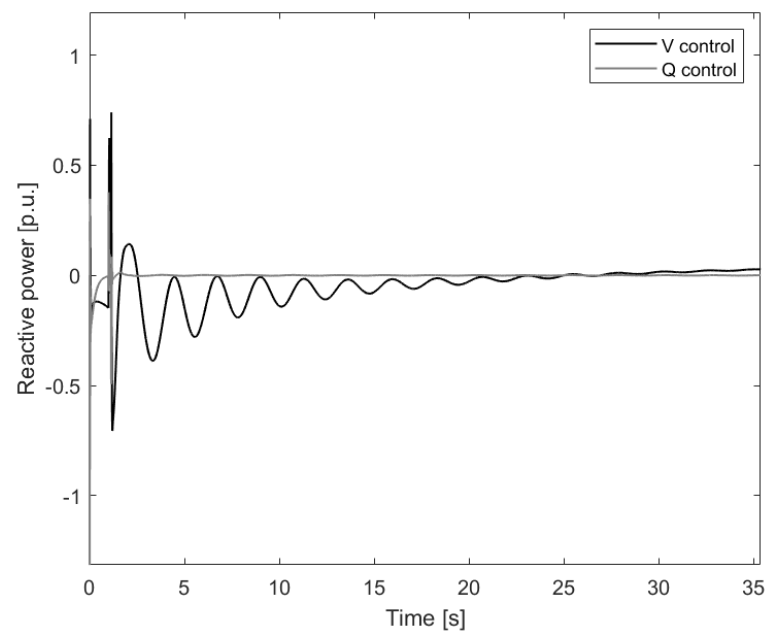


Figure 11. Reactive power provision from DFIGs in both V and Q control types.

Primary frequency support provision by the wind farm required the DFIGs to change their operating point from the optimal one in response to a frequency deviation. Figure 12 illustrates the active power provided by the DFIGs with and without frequency support during the first seconds after the occurrence of the fault. The DFIGs would normally be insensitive to the frequency deviations of the system. However, the droop control allowed them to respond to these deviations, improving the frequency stability of the system.

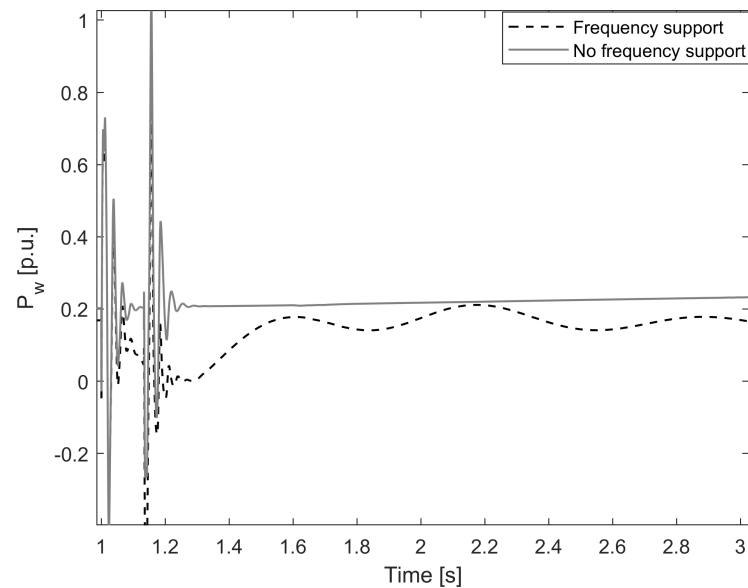


Figure 12. Active power from the wind farm with and without primary frequency support.

5.1.3. Scenario C (Displacement of G_4)

As pointed out by the authors of [13], a full characterization of the impacts of a wind farm should include both the addition of the wind farm and the displacement of part of the synchronous generation.

In this scenario, G_4 was displaced by the wind farm, as it was the closest synchronous generator to the wind farm location. In this way, the effect of wind integration on the power flows was minimized.

Table 3 shows that the addition of a wind farm, with the contextual displacement of a synchronous generator, led to a great improvement in both the local and inter-area mode damping. The damping ratio of the inter-area mode increased from $\zeta_{ia} = 3.30\%$ in the base case to about 12% when adding the wind farm and displacing G_4 . The damping of the dominant local mode almost doubled from $\zeta_l = 12.8\%$ to $\zeta_l = 21.5\%$. The effect on the converter control-based mode was similar to the previous scenario.

In this case, probably due to the missing primary frequency control of G_4 , the primary frequency support provision by the wind farm had a large beneficial effect on the damping ratio of the inter-area mode. Indeed, this scenario was the most damped one, where the damping ratio of the inter-area mode changed from the starting scenario without wind $\zeta_{ia} = 3.30\%$ to $\zeta_{ia} = 26.0\%$, as shown in Table 3 (dark gray bold values).

The change in damping can be visualized by zooming in on the complex plane around the region of the inter-area modes. Figure 13 illustrates the movement of the dominant inter-area mode toward a more stable region.

Although the primary frequency support provision improved the damping of electromechanical oscillations, it reduced the damping of the dominant converter control-based mode. However, since this mode was not an electromechanical one, it may not have largely affected the stability of the system as a whole. A time domain simulation was carried out to check the stability of the system, given the negative damping of the converter control-based dominant mode.

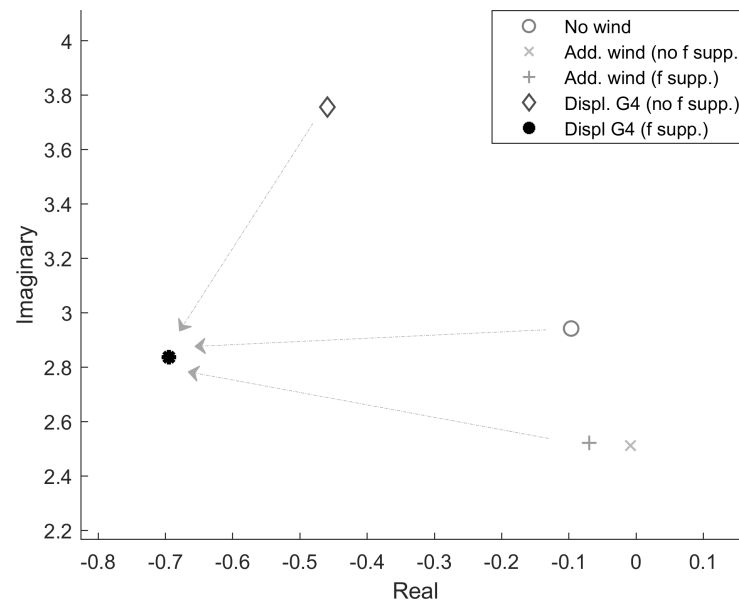


Figure 13. Graphical visualization of inter-area modes for different scenarios.

In Figure 14, the rotor speed of G_3 is compared for different scenarios. The one involving G_4 displacement led to larger oscillations due to the lacking inertia of the displaced synchronous generator. The figure shows how the primary frequency support resulted in a reduced amplitude of oscillations in this case. Additionally, Figure 14 shows that the slightly damped control mode did not seem to affect the stability of the system as a whole. However, this interesting link between the frequency support and converter controls requires further investigation, which is out of the scope of this paper.

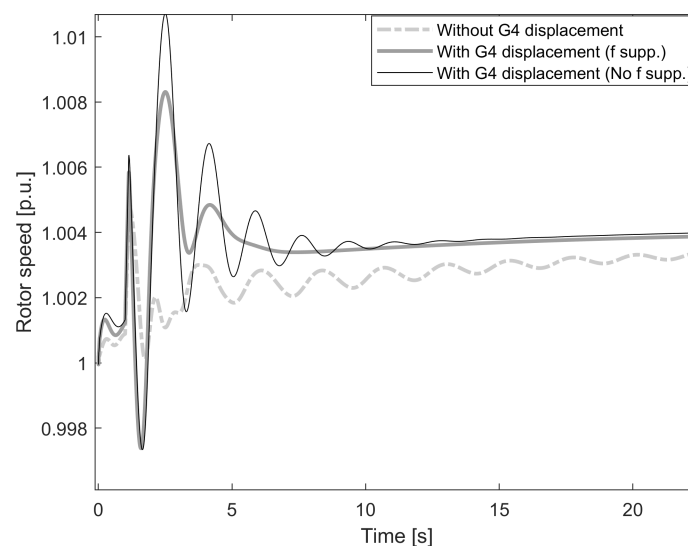


Figure 14. Rotor speed of generator G_3 with wind farm providing primary frequency response with and without displacement of G_4 .

As expected from the previous small-signal stability analysis, in the case with displacement of G_4 and frequency support, where $\zeta_{ia} = 26\%$, the oscillations were damped very quickly (i.e., in about 5 seconds). When no frequency support was provided, $\zeta_{ia} = 12.9\%$, and oscillations required about 15 s to be damped. If G_4 was not displaced, the frequency support still improved the damping of the system but to a smaller extent ($\zeta_{ia} = 2.80\%$), and the oscillations required more than 20 s to be damped.

An interesting aspect which is observable through the time domain simulations is the impact of the location of the input on the inertial and frequency support control. In the

previous analysis, a local signal was considered for the DFIGs. However, in the case of Wide-Area Monitoring Systems (WAMSs), control input signals could come from remote locations. Figure 15, representing the frequency support with a local signal or a remote signal from Area 1, shows that this may have an impact on the system.

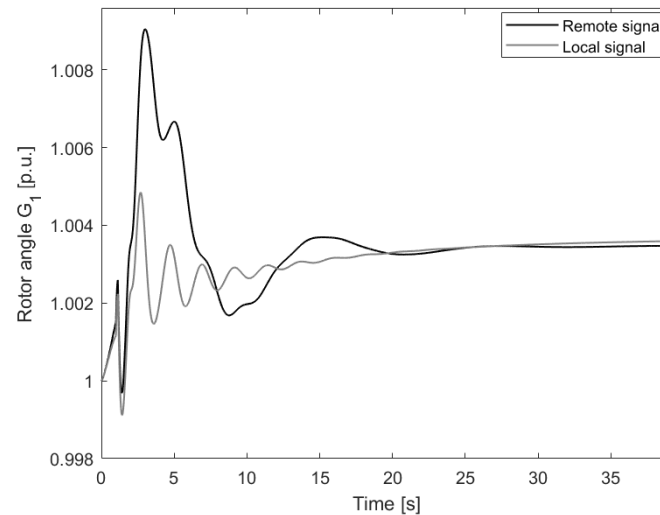


Figure 15. Effect of input signal location on the rotor angle of G_1 .

5.1.4. Discussion

The previous case studies demonstrated that frequency support provision, although implemented mainly to improve the frequency stability after a power imbalance, can provide a beneficial effect on the damping of electromechanical oscillations. The effects on the small-signal stability can be summarized as follows:

1. The damping of both local and inter-area oscillation modes improved when the wind farm provided primary frequency support. This effect was greater when a wind farm displaced part of the synchronous generation.
2. The dynamics of the wind farm became more intertwined with the inter-area and local oscillating modes. There was a less clear distinction between the converter and power system oscillating modes. Indeed, the CCBG-PI of λ_{cc} was lower, whereas the CCBG-PI associated with the local and inter-area modes increased.
3. The converter control-based mode became less damped with the displacement of G_4 . This phenomenon did not seem to affect the stability of the overall system, but it requires further investigation.

These results can be generalized to any values of the proportional gain K_p . Indeed, the value of K_p only affected the magnitude of the effect. Primary frequency support appeared to be beneficial for the inter-area and local modes and detrimental to the converter control-based mode, and the value of K_p only determined how beneficial or detrimental this effect was.

On the other hand, the sensitivity of the system to the inertial response provision was less straightforward. Different values of K_{in} can lead to either a beneficial or detrimental effect for each mode. The following paragraph provides a sensitivity analysis of both K_p and K_{in} .

5.2. Addition of Inertial Response and Sensitivity Analysis on Proportional Gains K_p and K_{in}

In this case study, the inertial response is included along with the primary frequency response, and the effect of both on low-frequency oscillations is discussed.

This analysis considered only the case with the addition of the wind farm, working in voltage control mode and without displacement of G_4 . The displacement of G_4 led to similar qualitative results, although the magnitude of the sensitivity changed.

The sensitivity analysis was carried out by calculating the dominant inter-area, local and control-based modes for a set of combinations of K_p and K_{in} , which varied in the range between 0 and 50 with a discrete step of 10. The total number of cases considered was 36, which was enough to draw the sensitivity curves of the eigenvalues on a complex plane.

Figure 16 shows how the dominant inter-area eigenvalue was affected by both the inertial and primary frequency responses.

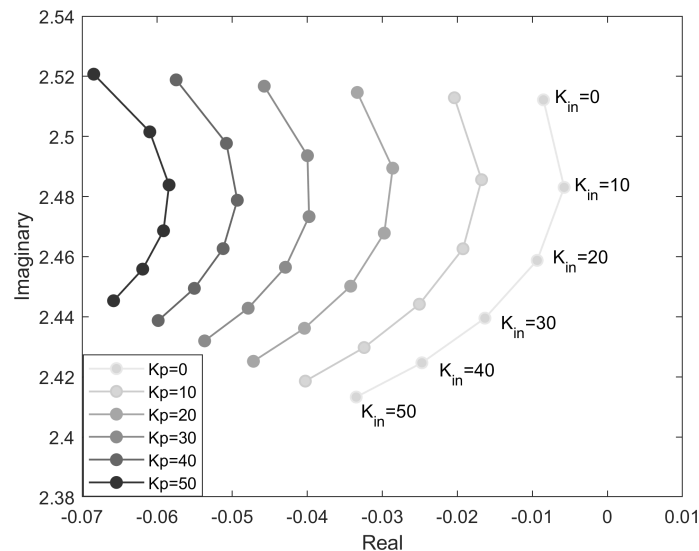


Figure 16. Sensitivity analysis of inter-area modes to K_p and K_{in} .

As previously outlined, higher K_p values led to progressively more damped modes. This was not true for the inertial response, since it could affect in a beneficial, detrimental or negligible way the inter-area mode, depending on the value of K_{in} . For lower values of K_p , the best damping was associated with $K_{in} = 50$. For larger values of K_p , the best damping was obtained for $K_{in} = 0$ (no inertial response) or $K_{in} = 50$. Intermediate values of K_{in} had a detrimental effect on damping in most cases.

Regarding the dominant local mode, it was very sensitive to K_{in} and K_p when their values were low (Figure 17). However, a certain degree of saturation can be observed for large values for both. For example, the changes to damping from $K_{in} = 40$ to $K_{in} = 50$ were negligible, as they were for K_p . In general, the inertial response seemed to have a detrimental effect on the dominant local mode. The highest damping was obtained when the inertial response was lacking ($K_{in} = 0$) and the primary frequency support was at its maximum ($K_p = 50$).

The converter control-based mode had an inverse behavior; its damping reduced with the increasing K_p value. The maximum damping was reached for $K_{in} = 10$ and $K_p = 0$ (Figure 18). It was highly sensitive to the inertial response provision in terms of frequency, and the imaginary component changed from 15 to 37 as K_{in} varied. The electromechanical modes showed much lower sensitivity.

As a final note, the inertial response seemed to affect mostly the imaginary component of the dominant modes (i.e., their frequencies), whereas the primary frequency response affected the real part to a higher extent, with little influence on the imaginary one.

In order to provide an idea of the behavior of generators with different inertial support gains, Figure 19 represents the time domain simulation for the case of $K_{in} = 20$ and $K_p = 50$.

These results highlight that inertial and primary frequency support provision can be beneficial to low-frequency oscillation damping. Furthermore, they stress the importance of optimal control systems' design for frequency support provision, which is required to mitigate possible associated negative impacts.

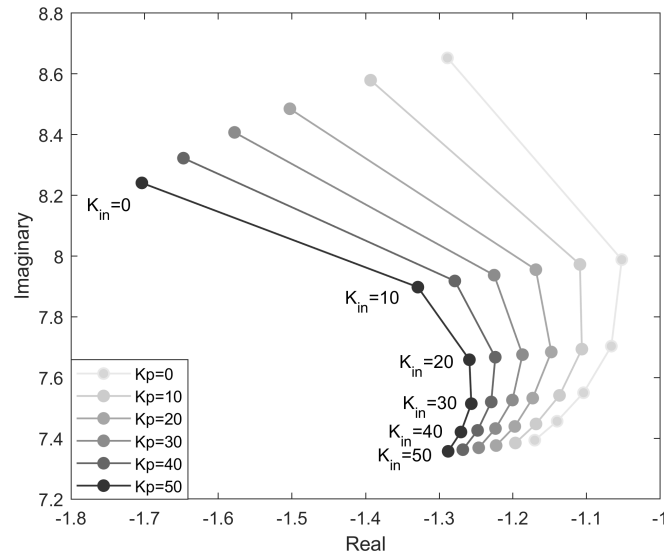


Figure 17. Sensitivity analysis of local modes to K_p and K_{in} .

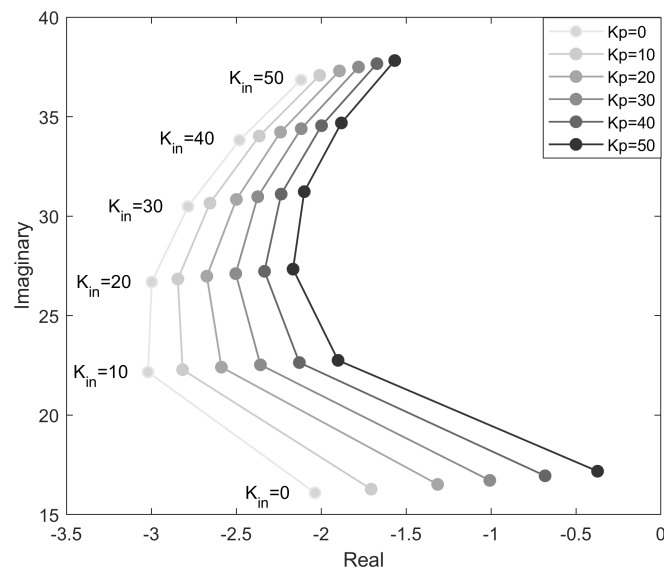


Figure 18. Sensitivity analysis of converter control-based modes to K_p and K_{in} .

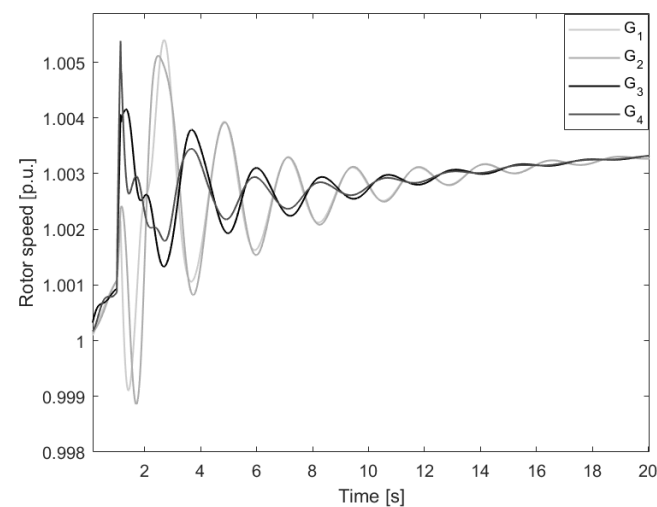


Figure 19. Time domain simulation for the case with $K_{in} = 20$ and $K_p = 50$.

6. Conclusions

In this paper, the effect of frequency support provision by DFIGs on low-frequency oscillation damping was investigated, with a discussion on both the electromechanical and converter control-based modes.

The analysis was divided into two parts.

First, the impact of the primary frequency response alone on the dominant inter-area, local and converter control-based modes was assessed. Small-signal stability analysis was carried out on the well-known two-area Kundur system while considering a total of nine scenarios. The resulting eigenvalue analysis was also substantiated by the results of the time domain simulations. Indeed, the modes observed through the small-signal stability analysis were excited by a three-phase fault on the tie line. The results showed that the primary frequency support provision by the wind farm had a beneficial effect on the damping of both the inter-area and local modes. The largest improvements were associated with the dominant inter-area mode, and the most damped scenario corresponded to the addition of the DFIGs, providing the primary frequency response, and the displacement of a synchronous generator. On the other hand, frequency support provision negatively affected the dominant converter control-based mode. From the results of a time domain simulation, this phenomenon did not seem to affect the stability of the whole system. However, it deserves more attention and will be explored in future work.

Finally, sensitivity analysis on the proportional gains K_p and K_{in} was conducted to assess the damping capabilities of DFIGs providing both inertial and primary frequency support. The results showed that, unlike the primary frequency support, the inertial response may either reduce damping or improve it, depending on the value of K_{in} and the considered mode.

These results demonstrate the importance of optimal control system design for frequency support provision, which should mitigate possible associated negative impacts and could provide an additional source of low-frequency oscillation damping.

Future works on the topic will be aimed at designing advanced and optimal controllers to provide both damping of low-frequency oscillations and frequency support in order to extend these results to a real large-scale system or to evaluate the impact of a wind farm's location.

Author Contributions: Conceptualization, A.P. and J.L.D.-G.; methodology, A.P. and J.L.D.-G.; software, A.P. and J.L.D.-G.; validation, A.P. and J.L.D.-G.; formal analysis, A.P. and J.L.D.-G.; investigation, A.P. and J.L.D.-G.; resources, A.P. and J.L.D.-G.; data curation, A.P. and J.L.D.-G.; writing—original draft preparation, A.P., J.L.D.-G. and A.V.; writing—review and editing, A.P., J.L.D.-G. and A.V.; visualization, A.P. and J.L.D.-G.; supervision, A.P., J.L.D.-G. and A.V. All authors have read and agreed to the published version of the manuscript.

Funding: This research received no external funding.

Data Availability Statement: Not applicable.

Conflicts of Interest: The authors declare no conflict of interest.

References

1. Ahmed, S.D.; Al-Ismael, F.S.; Shafiullah, M.; Al-Sulaiman, F.A.; El-Amin, I.M. Grid integration challenges of wind energy: A review. *IEEE Access* **2020**, *8*, 10857–10878. [[CrossRef](#)]
2. Milano, F.; Dörfler, F.; Hug, G.; Hill, D.J.; Verbič, G. Foundations and challenges of low-inertia systems. In Proceedings of the 2018 Power Systems Computation Conference (PSCC), Dublin, Ireland, 11–15 June 2018; pp. 1–25.
3. Attya, A.; Dominguez-Garcia, J.L.; Anaya-Lara, O. A review on frequency support provision by wind power plants: Current and future challenges. *Renew. Sustain. Energy Rev.* **2018**, *81*, 2071–2087. [[CrossRef](#)]
4. Díaz-González, F.; Hau, M.; Sumper, A.; Gomis-Bellmunt, O. Participation of wind power plants in system frequency control: Review of grid code requirements and control methods. *Renew. Sustain. Energy Rev.* **2014**, *34*, 551–564. [[CrossRef](#)]
5. Morren, J.; De Haan, S.W.; Kling, W.L.; Ferreira, J. Wind turbines emulating inertia and supporting primary frequency control. *IEEE Trans. Power Syst.* **2006**, *21*, 433–434. [[CrossRef](#)]

6. Chang-Chien, L.R.; Yin, Y.C. Strategies for operating wind power in a similar manner of conventional power plant. *IEEE Trans. Energy Convers.* **2009**, *24*, 926–934. [[CrossRef](#)]
7. Ruttledge, L.; Flynn, D. Emulated inertial response from wind turbines: Gain scheduling and resource coordination. *IEEE Trans. Power Syst.* **2015**, *31*, 3747–3755. [[CrossRef](#)]
8. Mahish, P.; Pradhan, A.K. Distributed synchronized control in grid integrated wind farms to improve primary frequency regulation. *IEEE Trans. Power Syst.* **2019**, *35*, 362–373. [[CrossRef](#)]
9. Ruttledge, L.; Miller, N.W.; O’Sullivan, J.; Flynn, D. Frequency response of power systems with variable speed wind turbines. *IEEE Trans. Sustain. Energy* **2012**, *3*, 683–691. [[CrossRef](#)]
10. Attya, A.B.T.; Dominguez-García, J.L. Insights on the provision of frequency support by wind power and the impact on energy systems. *IEEE Trans. Sustain. Energy* **2017**, *9*, 719–728. [[CrossRef](#)]
11. Tielens, P.; Van Hertem, D. The relevance of inertia in power systems. *Renew. Sustain. Energy Rev.* **2016**, *55*, 999–1009. [[CrossRef](#)]
12. Du, W.; Chen, X.; Wang, H. Strong dynamic interactions of grid-connected DFIGs with power systems caused by modal coupling. *IEEE Trans. Power Syst.* **2017**, *32*, 4386–4397. [[CrossRef](#)]
13. Du, W.; Bi, J.; Wang, H. Small-signal angular stability of power system as affected by grid-connected variable speed wind generators—A survey of recent representative works. *CSEE J. Power Energy Syst.* **2017**, *3*, 223–231. [[CrossRef](#)]
14. Gautam, D.; Vittal, V.; Harbour, T. Impact of increased penetration of DFIG-based wind turbine generators on transient and small signal stability of power systems. *IEEE Trans. Power Syst.* **2009**, *24*, 1426–1434. [[CrossRef](#)]
15. Vittal, E.; O’Malley, M.; Keane, A. Rotor angle stability with high penetrations of wind generation. *IEEE Trans. Power Syst.* **2011**, *27*, 353–362. [[CrossRef](#)]
16. Wilches-Bernal, F.; Chow, J.H.; Sanchez-Gasca, J.J. Impact of wind generation power electronic interface on power system inter-area oscillations. In Proceedings of the 2016 IEEE Power and Energy Society General Meeting (PESGM), Boston, MA, USA, 17–21 July 2016; pp. 1–5.
17. Du, W.; Bi, J.; Cao, J.; Wang, H. A method to examine the impact of grid connection of the DFIGs on power system electromechanical oscillation modes. *IEEE Trans. Power Syst.* **2015**, *31*, 3775–3784. [[CrossRef](#)]
18. Allen, A.J.; Singh, M.; Muljadi, E.; Santoso, S. Measurement-based investigation of inter-and intra-area effects of wind power plant integration. *Int. J. Electr. Power Energy Syst.* **2016**, *83*, 450–457. [[CrossRef](#)]
19. Domínguez-García, J.L.; Gomis-Bellmunt, O.; Bianchi, F.D.; Sumper, A. Power oscillation damping supported by wind power: A review. *Renew. Sustain. Energy Rev.* **2012**, *16*, 4994–5006. [[CrossRef](#)]
20. Surinkaew, T.; Ngamroo, I. Coordinated robust control of DFIG wind turbine and PSS for stabilization of power oscillations considering system uncertainties. *IEEE Trans. Sustain. Energy* **2014**, *5*, 823–833. [[CrossRef](#)]
21. Domínguez-García, J.L.; Ugalde-Loo, C.E.; Bianchi, F.; Gomis-Bellmunt, O. Input–output signal selection for damping of power system oscillations using wind power plants. *Int. J. Electr. Power Energy Syst.* **2014**, *58*, 75–84. [[CrossRef](#)]
22. Huang, J.; Yang, Z.; Yu, J.; Liu, J.; Xu, Y.; Wang, X. Optimization for DFIG fast frequency response with small-signal stability constraint. *IEEE Trans. Energy Convers.* **2021**, *36*, 2452–2462. [[CrossRef](#)]
23. Su, C.; Chen, Z. Influence of wind plant ancillary frequency control on system small-signal stability. In Proceedings of the 2012 IEEE Power and Energy Society General Meeting, San Diego, CA, USA, 22–26 July 2012; pp. 1–8.
24. Liu, H.; Yang, S.; Yuan, X. Inertia Control Strategy of DFIG-Based Wind Turbines Considering Low-Frequency Oscillation Suppression. *Energies* **2021**, *15*, 29. [[CrossRef](#)]
25. Hatziaargyriou, N.; Milanovic, J.; Rahmann, C.; Ajarapu, V.; Canizares, C.; Erlich, I.; Hill, D.; Hiskens, I.; Kamwa, I.; Pal, B.; et al. Definition and classification of power system stability revisited & extended. *IEEE Trans. Power Syst.* **2020**, *36*, 3271–3281.
26. Rogers, G. *Power System Oscillations*; Springer Science & Business Media: New York, NY, USA, 2012.
27. Quintero, J.; Vittal, V.; Heydt, G.T.; Zhang, H. The impact of increased penetration of converter control-based generators on power system modes of oscillation. *IEEE Trans. Power Syst.* **2014**, *29*, 2248–2256. [[CrossRef](#)]
28. Sloomweg, J.; De Haan, S.; Polinder, H.; Kling, W. General model for representing variable speed wind turbines in power system dynamics simulations. *IEEE Trans. Power Syst.* **2003**, *18*, 144–151. [[CrossRef](#)]
29. Van de Vyver, J.; De Kooning, J.D.; Meersman, B.; Vandeveld, L.; Vandoorn, T.L. Droop control as an alternative inertial response strategy for the synthetic inertia on wind turbines. *IEEE Trans. Power Syst.* **2015**, *31*, 1129–1138. [[CrossRef](#)]
30. Keung, P.K.; Li, P.; Banakar, H.; Ooi, B.T. Kinetic energy of wind-turbine generators for system frequency support. *IEEE Trans. Power Syst.* **2008**, *24*, 279–287. [[CrossRef](#)]
31. Attya, A.B.T.; Dominguez-García, J.L. A novel method to valorize frequency support procurement by wind power plants. *IEEE Trans. Sustain. Energy* **2019**, *11*, 239–249. [[CrossRef](#)]
32. Choi, J.W.; Heo, S.Y.; Kim, M.K. Hybrid operation strategy of wind energy storage system for power grid frequency regulation. *IET Gener. Transm. Distrib.* **2016**, *10*, 736–749. [[CrossRef](#)]
33. Kundur, P. *Power System Stability and Control*; CRC Press: New York, NY, USA, 2007.
34. Fu, Y.; Wang, Y.; Zhang, X. Integrated wind turbine controller with virtual inertia and primary frequency responses for grid dynamic frequency support. *IET Renew. Power Gener.* **2017**, *11*, 1129–1137. [[CrossRef](#)]
35. Rahimi, T.; Ding, L.; Kheshti, M.; Faraji, R.; Guerrero, J.M.; Tinajero, G.D.A. Inertia response coordination strategy of wind generators and hybrid energy storage and operation cost-based multi-objective optimizing of frequency control parameters. *IEEE Access* **2021**, *9*, 74684–74702. [[CrossRef](#)]

-
36. Zhao, J.; Lyu, X.; Fu, Y.; Hu, X.; Li, F. Coordinated microgrid frequency regulation based on DFIG variable coefficient using virtual inertia and primary frequency control. *IEEE Trans. Energy Convers.* **2016**, *31*, 833–845. [[CrossRef](#)]
 37. Slotweg, J.; Kling, W. Aggregated modelling of wind parks in power system dynamics simulations. In Proceedings of the 2003 IEEE Bologna Power Tech Conference Proceedings, Bologna, Italy, 23–26 June 2003; Volume 3, pp. 1–6.